Rhenium-188 Labeled Tungsten Disulfide Nanoflakes for Self-Sensitized, Near-Infrared Enhanced Radioisotope Therapy

Yu Chao, Guanglin Wang, Chao Liang, Xuan Yi, Xiaoyan Zhong, Jingjing Liu, Min Gao, Kai Yang, Liang Cheng,* and Zhuang Liu**

***R**adioisotope therapy (RIT), in which radioactive agents are administered or implanted into the body to irradiate tumors from the inside, is a clinically adopted cancer treatment method but still needs improvement to enhance its performances. Herein, it is found that polyethylene glycol (PEG) modified tungsten disulfide (WS_2) nanoflakes can be easily labeled by ^{188}Re, a widely used radioisotope for RIT, upon simple mixing. Like other high-Z elements acting as radiosensitizers, tungsten in the obtained ^{188}Re-WS_2-PEG would be able to absorb ionization radiation generated from ^{188}Re, enabling "self-sensitization" to enhance the efficacy of RIT as demonstrated in carefully designed in vitro experiments of this study. In the meanwhile, the strong NIR absorbance of WS_2-PEG could be utilized for NIR light-induced photothermal therapy (PTT), which if applied on tumors would be able to greatly relieve their hypoxia state and help to overcome hypoxia-associated radioresistance of tumors. Therefore, with ^{188}Re-WS_2-PEG as a multifunctional agent, which shows efficient passive tumor homing after intravenous injection, in vivo self-sensitized, NIR-enhanced RIT cancer treatment is realized, achieving excellent tumor killing efficacy in a mouse tumor model. This work presents a new concept of applying nanotechnology in RIT, by delivering radioisotopes into tumors, self-sensitizing the irradiation-induced cell damage, and modulating the tumor hypoxia state to further enhance the therapeutic outcomes.*

Y. Chao, C. Liang, J. Liu, M. Gao, Prof. L. Cheng, Prof. Z. Liu
Institute of Functional Nano and Soft Materials (FUNSOM)
Collaborative Innovation Center of Suzhou Nano Science and Technology
Soochow University
Suzhou, Jiangsu 215123, China
E-mail: lcheng2@suda.edu.cn; zliu@suda.edu.cn

G. Wang, X. Yi, X. Zhong, Prof. K. Yang
School of Radiation Medicine and Protection and School for Radiological and Interdisciplinary Sciences (RAD-X)
Collaborative Innovation Center of Radiation Medicine of Jiangsu Higher Education Institutions Medical College of Soochow University
Suzhou, Jiangsu 21513, China
E-mail: kyang@suda.edu.cn

DOI: 10.1002/smll.201601375

1. Introduction

Radiation therapy (RT) is a first-line treatment strategy for many types of cancers in the clinic.[1] There are two main kinds of radiation therapies, including external-beam radiation therapy (EBRT) and internal radioisotope therapy (RIT).[2] Unfortunately, in both types of RT, the damages of normal tissues can hardly be avoided.[3] Moreover, resistance often occurs during RT,[4] especially for tumors after multiple rounds of treatment,[5] as well as tumors with high levels of hypoxia (oxygen is required to enhance cell DNA damage caused by ionizing radiation in RT).[6] Developing effective methods to improve the therapeutic performances of RT is therefore of great importance.[7] Previously, radiolabeled tumor-homing nanoparticles[8] utilizing the enhanced permeability and retention (EPR) effect of cancerous

tumors[9] have been developed to improve cancer-targeted RIT.[10] On the other hand, nanoparticles containing high-Z elements have shown their capability to sensitize EBRT,[11] by absorbing ionizing-radiation beams (e.g., X-ray) to generate secondary charged particles such as Auger electrons to induce enhanced cancer cell killing.[12] However, whether tumor-homing radiolabeled nanoparticles containing high-Z elements would be able to self-sensitize RIT and improve its performance in cancer treatment, has not yet been discussed to our best knowledge.

Transition-metal dichalcogenides (TMDCs) have acquired widespread attention in recent years thanks to their unique structures and interesting physical/chemical properties.[13] With rather large specific surface area,[14] 2D TMDCs could act as biosensing platforms to detect various types of biological molecules,[15] or as drug delivery carriers with high drug loading efficiencies.[16] TMDCs with strong broad absorbance in the NIR region could also be used as photothermal agents for NIR-induced photothermal therapy (PTT).[17] Moreover, it has been uncovered by our group that TMDCs such as MoS_2 nanosheets may be labeled with radioisotope ions (e.g., $^{64}Cu^{2+}$) via a chelator-free method upon simple mixing, to enable position-emission tomography (PET) imaging.[18] In our latest work, we further demonstrated that tungsten disulfide (WS_2) nanoflakes with polyethylene glycol (PEG) coating could be used to sensitize external radiotherapy induced by X-ray.[19]

Motivated by our series of studies with TMDCs, herein, we hypothesize that PEGylated WS_2 nanoflakes may also be labeled with an RIT radioisotope via the chelator-free method,[20] and enhance the RIT-induced cancer cell damage via a new mechanism of "self-sensitization". ^{188}Re is a commonly used RIT radioisotope that emit both beta and gamma rays during its decay (half-life = 16.9 h).[21] and shows strong binding with oxygen and sulfur atoms.[22] After being reduced from $^{188}Re^{VII}O_4^-$, the obtained $^{188}Re^{IV}$ ions could be directly labeled on PEGylated WS_2 nanoflakes via the chelator-free method to afford ^{188}Re-WS_2-PEG with high radiolabeling stability. As evidenced by carefully designed in vitro experiments, WS_2 nanoflakes containing the high-Z element, tungsten, are able to enhance ^{188}Re-induced cell damage, likely via interacting with the radioactive irradiation emitted from ^{188}Re anchored on the surface of WS_2. In addition to such "self-sensitization" mechanism, it is further uncovered that the NIR-induced in vivo mild photothermal heating of tumors with WS_2-PEG is able to greatly relieve the tumor hypoxia state possibly by promoting intratumoral blood flow, overcoming hypoxia-associated radiation resistance of tumors.[23] Those effects acting together may contribute to the remarkably enhanced therapeutic efficacy of RIT delivered by ^{188}Re-WS_2-PEG.

2. Results and Discussion

The synthesis, modification, and ^{188}Re radiolabeling of WS_2 nanoflakes are illustrated in **Figure 1**a. In brief, WS_2 nanoflakes were prepared using a high-temperature solution method by reacting WCl_6 with sulfur dissolved in a mixed solvent of oleylamine (OM) and 1-octadecene (ODE) at 300 °C under N_2 atmosphere for 30 min (Figure S1, Supporting Information).[24] An amphiphilic polymer, poly(ethylene glycol) (PEG) grafted poly (maleic anhydride-alt-1-octadecene) (C_{18}PMH-PEG), was used to transfer as-made hydrophobic WS_2 nanoflakes into the aqueous phase by ultrasonication. After modification, the obtained WS_2-PEG nanoflakes showed largely reduced sizes to the range of 80–150 nm as revealed by transmission electron microscopy (TEM; Figure 1b).[17a] Notably, such PEGylated nanoflakes exhibited high stability in various physiological solutions without aggregation (Figure S2, Supporting Information).

UV–vis–NIR spectrum of WS_2-PEG revealed strong absorbance in the NIR region (Figure 1c). The mass extinction coefficient of WS_2-PEG nanoflakes was 23.8 $Lg^{-1}cm^{-1}$ as reported,[17a] which was much higher than that of graphene oxide (GO, 3.6 $Lg^{-1}cm^{-1}$) and similar with reduced GO (24.6 $Lg^{-1}cm^{-1}$).[25] As expected, WS_2-PEG showed great photothermal heating efficiency by a concentration-dependent manner (Figure 1d), allowing its application for NIR-induced PTT.

For the radiolabeling of WS_2-PEG nanoflakes, we mixed WS_2-PEG with radioactive rhenium-188 (^{188}Re) precursor, sodium perrhenate ^{188}Re ($Na^{188}ReO_4$), in the presence of stannous chloride ($SnCl_2$), which could reduce $^{188}Re^{VII}$ in $Na^{188}ReO_4$ into $^{188}Re^{IV}$ ions.[26] Similar to the chelator-free labeling of MoS_2 with $^{64}Cu^{2+}$ as reported in our previous work,[18] it was found that $^{188}Re^{IV}$ ions could also be anchored on the surface of WS_2 possibly at the W defect sites on WS_2 by bonding with sulfur atoms, without the need of any chelators. After removal of excess free ^{188}Re by ultrafiltration, the radiolabeling yield was determined to be as high as 95 ± 1.34% as measured by the γ-counter. The radiolabeling stability of ^{188}Re labeled WS_2-PEG was then tested by incubating the obtained ^{188}Re-WS_2-PEG nanoflakes in phosphate buffered saline (PBS) or serum at 37 °C for 24 h. Little detachment of ^{188}Re from the radiolabeled ^{188}Re-WS_2-PEG was observed, suggesting the high stability of ^{188}Re labeling on WS_2-PEG nanoflakes by such a simple chelator-free method (Figure 1e). To investigate the prolonged colloidal stability, WS_2-PEG nanoflakes labeled with "cold" non-radioactive Re were incubated with various physiological solutions including PBS and fetal bovine serum for 3 d. The dynamic light scattering (DLS) results showed that Re-WS_2-PEG exhibited great stability in various physiological solutions (Figure S3, Supporting Information).

Previously we have reported that WS_2 could act as a radiosensitizer to enhance EBRT by absorbing X-ray.[19,27] We thus wondered whether there would be a "self-sensitizing" mechanism if ^{188}Re-WS_2-PEG nanoflakes were used for RIT (**Figure 2**a,c). It was found that 4T1 murine breast cancer cells incubated with ^{188}Re-WS_2-PEG for 24 h showed high radioactivity as measured by the gamma counter, compared with that incubated with free ^{188}Re (Figure S4, Supporting Information). In the meanwhile, confocal fluorescence images of cells incubated with Cy5.5 labeled WS_2-PEG illustrated strong fluorescence signals in the cytoplasm, also indicating obvious cell uptake of WS_2-PEG (Figure S5, Supporting Information). In our in vitro experiments, 4T1

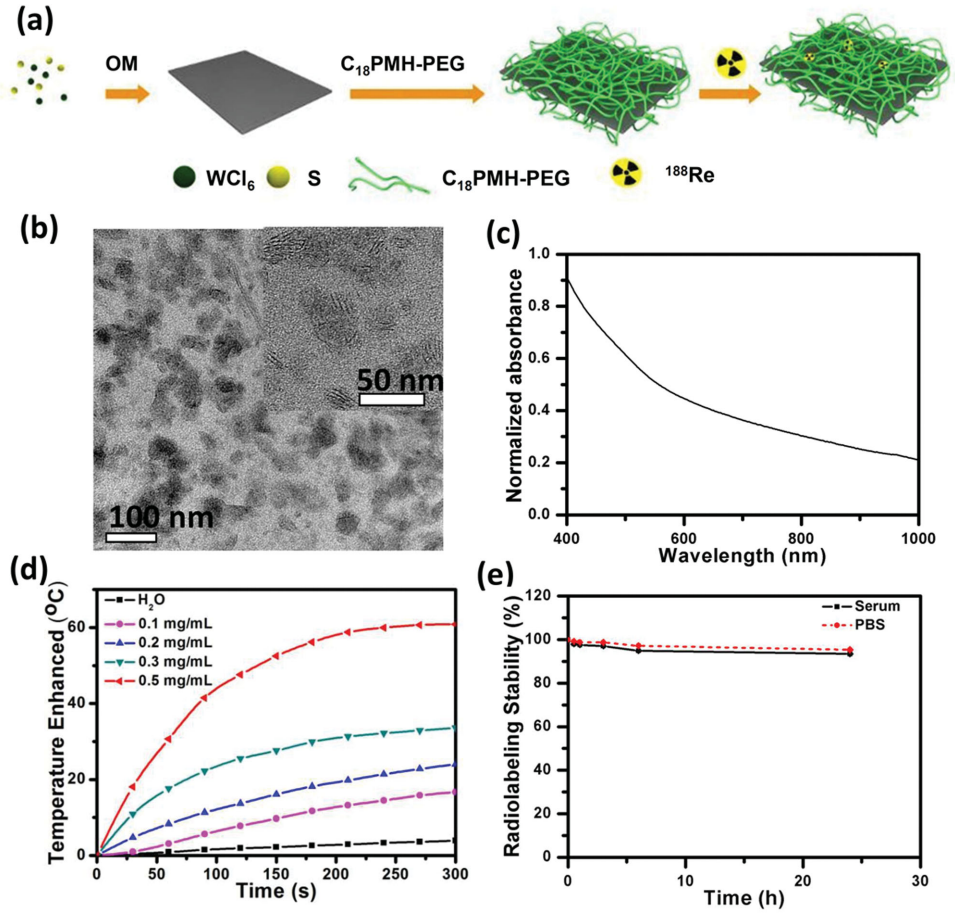

Figure 1. WS_2-PEG synthesis and characterization. a) A scheme of synthesis and modification of WS_2 nanoflakes and radiolabeling of ^{188}Re. b) TEM images of PEGylated WS_2 nanoflakes. Inset: A higher resolution TEM image. c) UV–vis–NIR absorbance spectra of WS_2-PEG in water. d) The photothermal heating curves of water and WS_2-PEG with different concentrations (0.1, 0.2, 0.3, and 0.5 mg mL^{-1}) under 808-nm laser at 0.8 W cm^{-2} for 5 min. e) Radiolabeling Stability of ^{188}Re radiolabeled WS_2-PEG in PBS and serum.

cancer cells were pre-incubated with "cold" WS_2-PEG without radiolabeling at different concentrations (0, 0.025, 0.05, and 0.1 mg mL^{-1}) for 24 h, washed with PBS to remove un-internalized WS_2-PEG, and then re-incubated in fresh cell culture containing different doses of free ^{188}Re at 0, 1.25, 2.5, 5, 10, 20, 40, 80, 160, and 320 μCi mL^{-1} for 24 h. After that, the cell counting kit-8 (CCK8) assay was carried out to determine the relative cell viabilities. Compared to cells without pretreating by WS_2-PEG, cells pretreated with WS_2-PEG showed significantly enhanced RIT-induced cell damage at the same radioactive doses (Figure 2b), despite the no appreciable cytotoxicity of WS_2-PEG towards those cells. Therefore, our results indicated that WS_2-PEG has the sensitization capability not only for X-ray-induced EBRT, but also to enhance radioisotope-induced RIT. In particular, for ^{188}Re with both β-ray and γ-ray emission during its decay, while its emitted β-ray (electrons) would directly cause cell damage, its γ-ray, which otherwise would be largely ineffective to cells (at the used RIT dose), may be partially adsorbed by WS_2 to produce charged secondary particles and destruct tumor cells.[11a,28]

Next, we emulated the in vitro cancer cell killing efficacy of ^{188}Re-WS_2-PEG, in which ^{188}Re is a radioemitter and WS_2 is a radiosensitizer so that both β-ray and γ-ray emission from ^{188}Re-WS_2-PEG may be effectively utilized for cancer killing. 4T1 cells were incubated with different concentrations of WS_2-PEG, free ^{188}Re, or ^{188}Re-WS_2-PEG for 24 h and then tested by the CCK8 assay. No significant cytotoxicity was observed for WS_2-PEG nanoflakes even at high concentration up to 0.1 mg mL^{-1}. ^{188}Re-WS_2-PEG showed significantly enhanced RIT-induced cancer cell damage compared to free ^{188}Re at the same radioactivity doses (Figure 2d), likely owing to the "self-sensitization" mechanism as well as the enhanced cellular uptake of radioisotopes once loaded on the WS_2 nanocarrier (Figure S4, Supporting Information). Thus, ^{188}Re-WS_2-PEG appeared to be a rather effective agent for RIT.

^{188}Re labeling of WS_2-PEG nanoflakes not only enabled enhanced RIT, but also allowed us to quantitatively track the in vivo behaviors of those nanoflakes after they were administered into animals. Female BALB/C mice-bearing 4T1 tumors were intravenously (i.v.) injected with ^{188}Re-WS_2-PEG (20 mg kg^{-1}, 1 mCi) and then scanned under single photoemission-computed tomography (SPECT) imaging. Being widely distributed throughout the mouse body right after injection of ^{188}Re-WS_2-PEG, high levels of radioactivity accumulation were observed in the liver, spleen, and tumor at 24 h post injection (p.i.) (**Figure 3**a). We next quantitatively

Materials Views
www.MaterialsViews.com

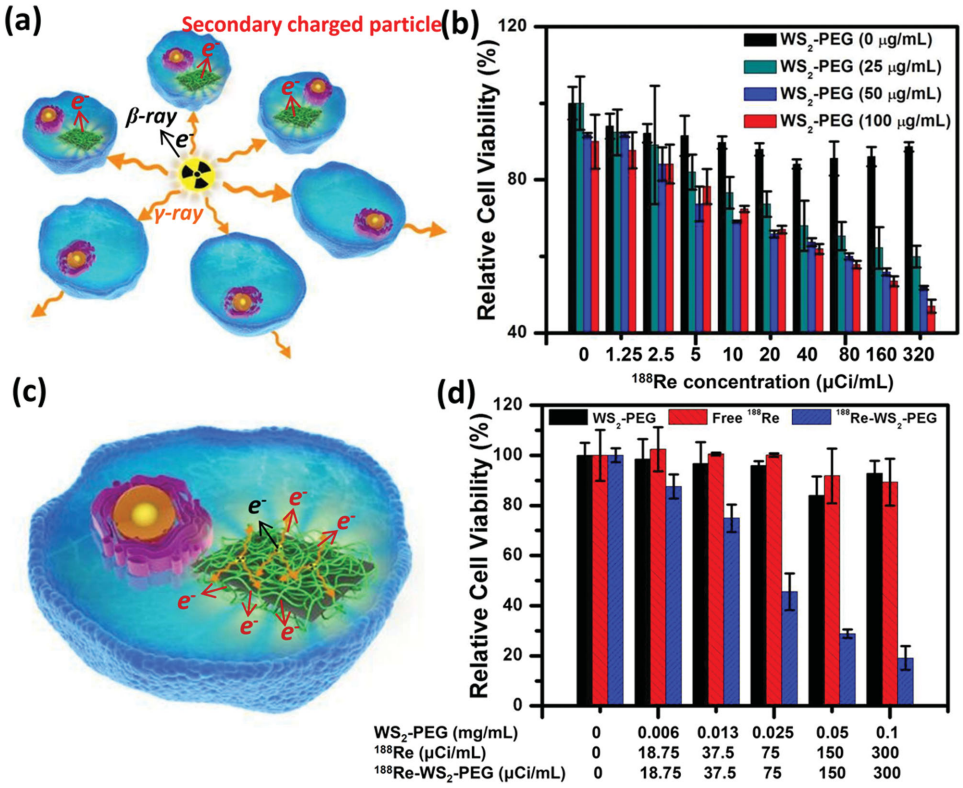

Figure 2. In vitro cell experiment. a) A scheme showing the proposed mechanism of enhanced ^{188}Re-induced cancer cell killing by WS_2-PEG. b) Relative viabilities of 4T1 cells pretreated with different concentrations of WS_2-PEG (0, 25, 50, and 100 μg mL^{-1}) after incubated with free ^{188}Re for 24 h. The RIT effect of free ^{188}Re could be enhanced by WS_2-PEG. c) A scheme showing the proposed mechanism of the "self-sensitizing" effect by ^{188}Re-WS_2-PEG inside cells. d) Relative viabilities of 4T1 cells incubated with WS_2-PEG, free ^{188}Re and ^{188}Re-WS_2-PEG with different concentrations for 24 h. We used the same WS_2 concentrations in our experiments for WS_2-PEG and ^{188}Re-WS_2-PEG. ^{188}Re-WS_2-PEG showed much stronger RIT effect compared to free ^{188}Re at the same doses.

studied the in vivo behaviors of ^{188}Re-WS_2-PEG by ex vivo measurement of radioactivities. Six female BALB/C mice were i.v. injected with ^{188}Re-WS_2-PEG or free ^{188}Re, with their blood collected at varied time points. By measuring radioactivity counts in blood samples using a gamma counter, the blood circulation behaviors of ^{188}Re-WS_2-PEG, and free ^{188}Re could be determined. Compared with free ^{188}Re, ^{188}Re-WS_2-PEG nanoflakes exhibited greatly prolonged blood circulation, with the blood half-life determined to be ≈3.22 h (Figure 3b). For biodistribution measurement, mice-bearing 4T1 tumors were i.v. injected with ^{188}Re-WS_2-PEG or free ^{188}Re and sacrificed at 24 h p.i. to collect main tissues and organs for gamma counting. Consistent with SPECT imaging data, high levels of ^{188}Re-WS_2-PEG uptake in the liver, spleen, and tumor were observed, whereas little retention of free ^{188}Re was observed in various organs of mice due to its fast excretion (Figure 3c).The high tumor uptake up to ≈10% of injected dose per gram tissue (%ID g^{-1}) should be attributed to the EPR effect of tumors to allow passive homing of nanostructures with long blood circulation half-lives.

WS_2-PEG with strong NIR absorbance could be utilized as a photothermal heater under NIR laser exposure. We then tested the photothermal tumor heating with WS_2-PEG under a low-power NIR laser irradiation and studied the impact of such mild hyperthermia treatment to tumors. At 24 h post i.v. injection of WS_2-PEG (dose = 20 mg kg^{-1}), 4T1 tumor-bearing mice were exposed to an 808-nm NIR laser at the power density of 0.2–0.3 W cm^{-2} for 20 min. As revealed by infrared imaging camera (**Figure 4**a), the tumor surface temperature was maintained at 44–45 °C during laser irradiation for mice injected with WS_2-PEG nanoflakes, whereas the heating for saline injected mice was much weaker (≈37 °C) (Figure 4b). It is known that a mild hyperthermia treatment that is insufficient to directly ablate tumors may be able to enhance the intra-tumor blood flow and improve tumor oxygenation.[6a,11c] Immunofluorescence hypoxia staining assay was thus carried out for tumor slices following the standard protocol (Figure 4c).[29] Compared with control group with WS_2-PEG injection but no NIR laser irradiation, NIR irradiation of tumors on mice injected with WS_2-PEG resulted in significantly decreased pimonidazole-stained (green) hypoxic area (Figure 4d), indicating that the mild photothermal heating could effectively relieve the hypoxia state of tumors.

The in vivo therapeutic efficacy with ^{188}Re-WS_2-PEG was then evaluated with the 4T1 tumor model. There were six-group mice for in vivo treatment (five mice per group): control, WS_2-PEG, WS_2-PEG + laser, free ^{188}Re, ^{188}Re-WS_2-PEG, and ^{188}Re-WS_2-PEG + laser (dose of WS_2-PEG = 20 mg kg^{-1}, ^{188}Re = 200 μCi per mouse). Laser irradiation was conducted 24 h post i.v. injection of various agents using the 808-nm laser at the power density of ≈0.3 W cm^{-2} for 20 min. Compared to free ^{188}Re which at the current dose showed no appreciable

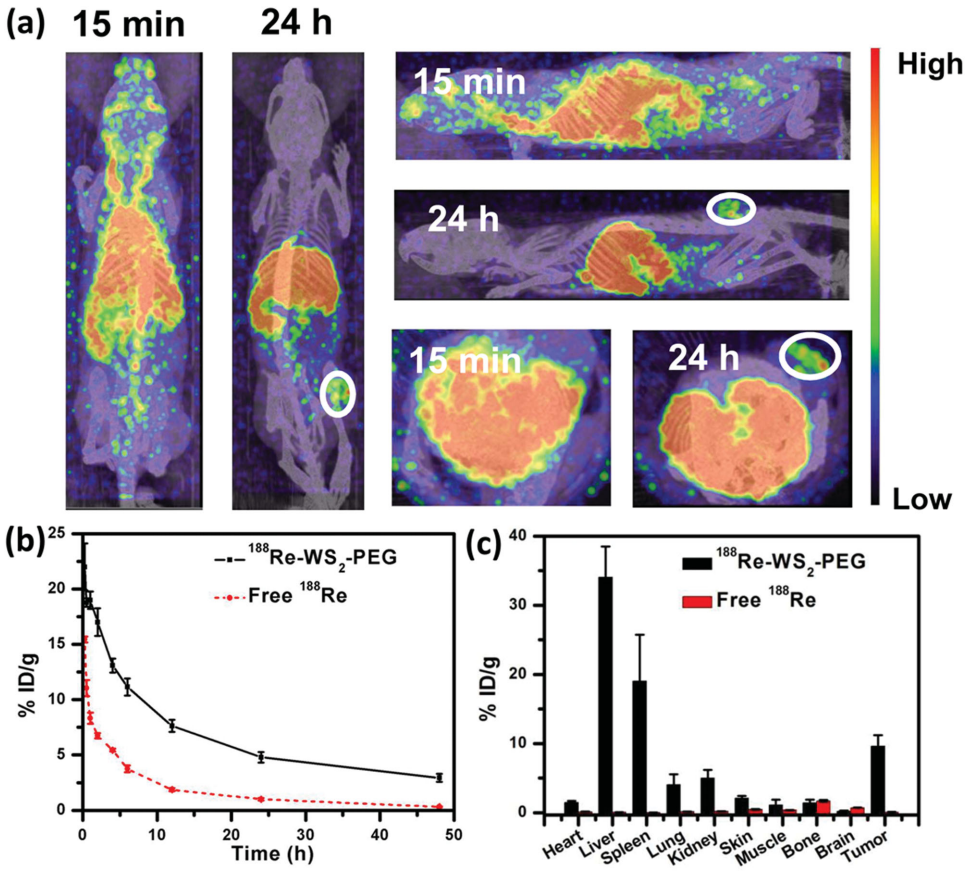

Figure 3. In vivo imaging and pharmacokinetics. a) SPECT images of 4T1 tumor-bearing mice after i.v. injection with ^{188}Re-WS$_2$-PEG. b) The blood circulation of free ^{188}Re and ^{188}Re-WS$_2$-PEG in mice post i.v. injection. c) Biodistribution of free ^{188}Re and ^{188}Re-WS$_2$-PEG measured at 24 h post i.v. injection. Efficient tumor uptake of ^{188}Re-WS$_2$-PEG was observed.

inhibitory effect to the tumor growth, ^{188}Re-WS$_2$-PEG nanoflakes treatment could obviously delay the tumor growth, particularly in the early three days post treatment (**Figure 5**a), likely owing to the enhanced tumor accumulation of ^{188}Re loaded on those nanoflakes, as well as the "self-sensitization" mechanism that made ^{188}Re-WS$_2$-PEG to be a more effective RIT agent. Unfortunately, tumors in this group still grew up later. Similarly, photothermal heating of tumors with unlabeled WS$_2$-PEG at the used mild condition also could only partially delay the tumor growth (Figure 5a). Excitingly, for mice treated with ^{188}Re-WS$_2$-PEG plus NIR-induced photothermal heating, their tumors were completely eliminated (disappeared at 6 d p.i. for all five mice) (Figure 5a). Notably, all the five mice receiving NIR-enhanced RIT with ^{188}Re-WS$_2$-PEG were tumor-free after treatment and survived for more than two months, whereas mice in the control groups showed life spans of 16–20 d for untreated or free ^{188}Re treated mice, and 22–30 d for mice receiving RIT alone with ^{188}Re-WS$_2$-PEG or PTT alone with cold WS$_2$-PEG (Figure 5b).

In order to verify the observed therapeutic effects, tumors from mice after various treatments were collected two days after treatment. For tumors on mice after treatment by NIR-enhanced RIT with ^{188}Re-WS$_2$-PEG, significant tumor cell damage and obviously enhanced apoptosis were observed by Haematoxylin and Eosin (H&E) and Terminal deoxynucleotidyl transferase dUTP nick end labeling (TUNEL) staining, respectively, in marked comparison to the other control groups (Figure 5c,d). Our results collectively evidenced the superior anti-tumor therapeutic effect achieved by ^{188}Re-WS$_2$-PEG with the help of NIR laser irradiation.

Notably, treatment with WS$_2$-PEG or ^{188}Re-WS$_2$-PEG induced no obvious body weight change to treated mice (20 mg kg^{-1} of WS$_2$-PEG corresponding to 200 μCi of ^{188}Re), indicating no significant acute toxicity of RIT delivered by ^{188}Re-WS$_2$-PEG (Figure S6, Supporting Information). To look into the possible side effects of such treatment, main organs including heart, liver, spleen, lung, and kidney from the ^{188}Re-WS$_2$-PEG treated mice were then examined at the end of treatment (day 60) by H&E staining. No significant organ damage or abnormality was observed (Figure S7, Supporting Information), suggesting the limited long-term toxicity of ^{188}Re-WS$_2$-PEG to the treated mice. Considering the no appreciable in vivo toxicity of WS$_2$-PEG observed in our previous more systematic toxicology studies, as well as the short decay half-life of ^{188}Re, such ^{188}Re-WS$_2$-PEG agent may be a relatively safe agent for application in RIT.

3. Conclusion

In summary, WS$_2$-PEG nanoflakes were labeled with ^{188}Re, a commonly used RIT radioisotope, with rather high labeling

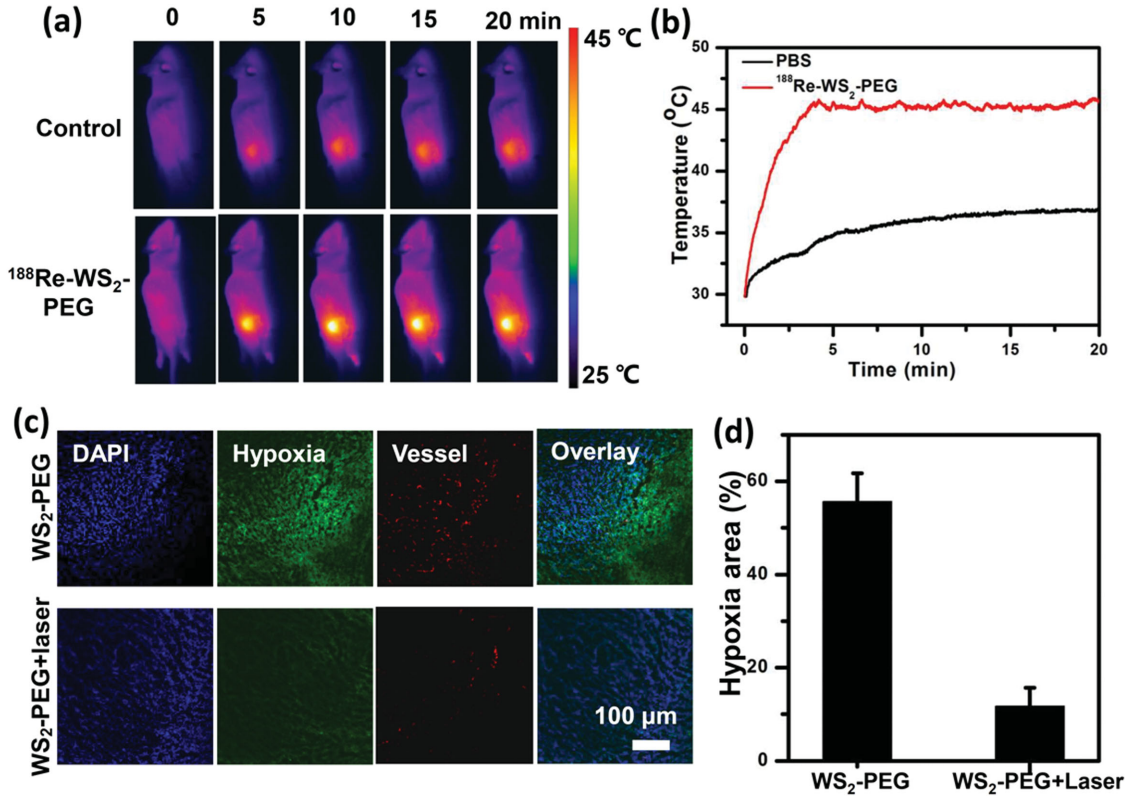

Figure 4. NIR-induced PTT on tumor hypoxia. a) IR thermal images of 4T1 tumor-bear mice under the 808-nm laser irradiation (0.2–0.3 W cm^{-2}) 24 h after i.v. injection of saline or WS_2-PEG (dose = 20 mg kg^{-1}). b) Temperature-heating curves of tumors after irradiation for 20 min for mice in (a). c) Representative immunofluorescence images of tumor slices with hypoxia staining. Cell nuclei, blood vessels, and hypoxia areas were stained by DAPI (blue), anti-CD31 (red), and anti-pimonidazole (green), respectively. d) Ratio of relative hypoxia areas for tumors in different groups shown in (c).

efficiency (≈95%) and great stability, via a chelator-free method upon simple mixing. Interesting, we for the first time proposed a "self-sensitization" mechanism in RIT with the obtained ^{188}Re-WS_2-PEG, in which the emitted radioactive γ-radiation from ^{188}Re could be absorbed by W to generate secondary electrons to enhance radiation-induced damage to cancer cells, a mechanism similar to that reported when high-Z element agents are used to sensitize EBRT by absorbing X-ray. As the result of such "self-sensitization" behavior as well as enhanced cellular uptake of ^{188}Re once binding on WS_2-PEG, ^{188}Re-WS_2-PEG showed dramatically improved in vitro cancer cell killing efficacy compared to free ^{188}Re. We further utilized the gamma emission of ^{188}Re to track the in vivo behaviors of ^{188}Re-WS_2-PEG by in vivo SPECT imaging and ex vivo biodistribution measurement, which both uncovered efficient passive tumor homing of those nanoflakes by the EPR effect. With high NIR absorbance, ^{188}Re-WS_2-PEG could act as a photothermal agent to heat up tumors under NIR laser exposure, resulting in greatly promoted tumor oxygenation which would be favorable for overcoming hypoxia-associated radiotherapy resistance. Therefore, in vivo NIR-enhanced RIT with ^{188}Re-WS_2-PEG was finally realized, offering a remarkably improved therapeutic outcome with a rather low radioactivity dose, at which free ^{188}Re appeared to be essentially ineffective. This work presents a novel strategy to enhance RIT cancer treatment with nanotechnology utilizing TMDC nanomaterials. For future clinical translation of such technology, efforts may still be needed to develop biodegradable/rapid-execrable agents to realize similar aims.

4. Experimental Section

Synthesis of WS_2 Nanoflakes: All materials used in this work were obtained from Sigma–Aldrich, unless indicated. Na $^{188}ReO_4$ radiopharmaceutical was provided by Atomic firm Sinovac Pharmaceutical Co. LTD., Shanghai. WS_2 nanoflakes were synthesized following our previous process by a bottom-up method.[24] In brief, OM (15 mL), and ODE (10 mL) were mixed in a three-necked flask (50 mL) at room temperature, and then Tungsten chloride (WCl_6) (1 mmol) was added. The reaction solution was heated to 140 °C to remove water and oxygen for 30 min under the protection of nitrogen with vigorous magnetic stirring. After that, the whole system was heated up to 300 °C and then immediately added with sulfur (2 mmol, dissolved in 4 mL OM). The reaction was kept at this state about 30 min. After cooling down to room temperature, WS_2 nanaoflakes were washed with ethanol and cyclohexane for three times, and then collected by centrifugation.

Modification of WS_2 Nanoflakes: PEG grafted poly-(maleic anhydride-alt-1-octadecene) (C_{18}PMH-PEG_{5K}) and Amine-PEG grafted C_{18}PMH (C_{18}PMH-PEG_{5K}-NH_2) were synthetized according to our previous protocols.[30] For surface modification, 20 mg as-made WS_2 nanoflakes were dispersed in 5 mL trichloromethane ($CHCl_3$) containing 200 mg C_{18}PMH-PEG or C_{18}PMH-PEG-NH_2. After 6 h stirring, the solution was dried by nitrogen and dissolved in

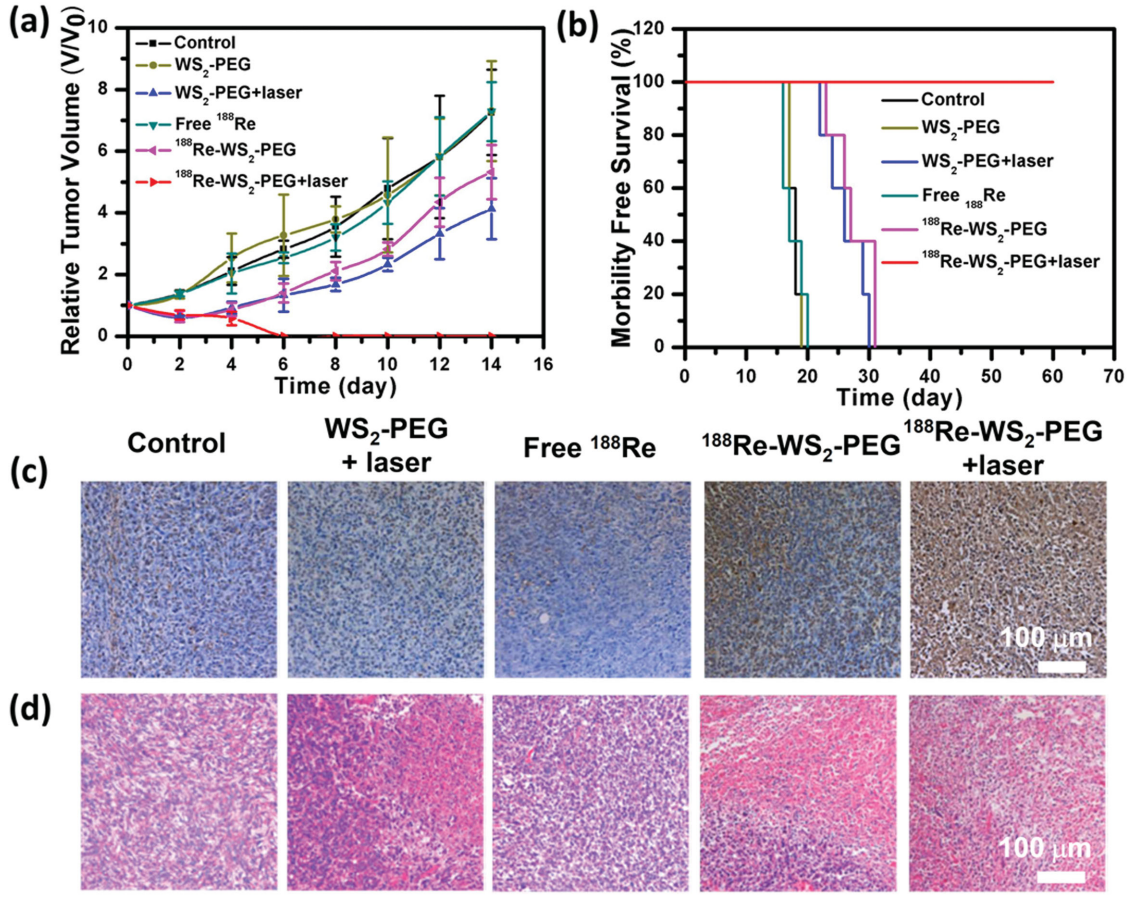

Figure 5. NIR-enhanced RIT delivered by ^{188}Re-WS_2-PEG. a,b) Relative tumor volumes (a) and survival rate of mice (b) after different treatments indicated including PBS control, WS_2-PEG injection with laser irradiation, free ^{188}Re injection, as well as ^{188}Re-WS_2-PEG injection without and with laser irradiation. c,d) Representative TUNEL (c) and H&E (d) stained tumor slices from six groups. The tumors were collected one day post various treatments were conducted.

water. After removal of excess coating polymers by centrifugation, the final product was stored at 4 °C for further use. WS_2 nanoflakes were modified with C_{18}PMH-PEG_{5K}-NH_2 to allow fluorescent labeling with N-hydroxysuccinimide ester modified Cy5.5 (NHS-Cy5.5).

Characterization: TEM images were obtained by a FEI Tecnai F20 transmission electron microscope at an acceleration voltage of 200 KV. DLS of WS_2-PEG nanoflakes was obtained by a Zetasizer Nano-ZS (Malvern Instruments, UK). UV–vis–NIR spectra of WS_2-PEG in water were recorded by PerkinElmer Lambda 750 UV–vis–NIR spectrophotometer (PL).

^{188}Re Radiolabeling: Radioactive rhenium-188 (^{188}Re) precursor, Na $^{188}ReO_4$, was reduced from $^{188}Re^{VII}$ to $^{188}Re^{IV}$ by stannous chloride ($SnCl_2$).[22a] First, 200 μL WS_2-PEG (2 mg mL^{-1}), 100 μL ascorbic acid (2 mg mL^{-1}) and $SnCl_2$ (10 mg mL^{-1}) were mixed in a 2 mL tube. Then, 200 μL Na $^{188}ReO_4$ solution was added into the tube and then blended. The solution pH was kept at ≈4 during this labeling reaction at 37 °C. After 1 h, the solution was washed for three times by ultrafiltration filters with molecular weight cutoff of 100 kDa. The final product was ^{188}Re-WS_2-PEG. In order to confirm the stability of radiolabeled ^{188}Re-WS_2-PEG, ^{188}Re-WS_2-PEG was incubated with PBS or serum at 37 °C for different periods of time (0.5, 1, 3, 6, and 24 h). After that, the released ^{188}Re from ^{188}Re-WS_2-PEG was collected by ultrafiltration for gamma counting to determine the amount of retained ^{188}Re on the labeled nanoflakes.

Cell Experiments: 4T1 murine breast cancer cells were obtained from American Type Culture Collection and cultured in the standard medium. To study the "self-sensitizing" mechanism, 4T1 cells were pre-incubated with "cold" WS_2-PEG without radiolabeling at different concentrations (0, 0.025, 0.05, and 0.1 mg mL^{-1}) for 24 h, washed with PBS to remove un-internalized WS_2-PEG, and then re-incubated in fresh cell culture added with different concentrations of free ^{188}Re at 0, 1.25, 2.5, 5, 10, 20, 40, 80, 160, and 320 μCi mL^{-1} for 24 h. Relative cell viabilities were determined by the CCK-8 assay. For in vitro cancer cell killing induced by RIT, 4T1 cells were incubated with different concentrations of WS_2-PEG, free ^{188}Re, and ^{188}Re-WS_2-PEG for 24 h. After that, CCK8 assay was carried out. To determine the cellular uptake of ^{188}Re, 4T1 cells were pre-seeded in six well plates at the density of 2×10^5 cells per well and incubated with different concentrations of free ^{188}Re and ^{188}Re-WS_2-PEG at 5, 10, 20, 40, and 80 μCi for 24 h. After washing cells with PBS for three times, cells were collected for gamma counting to measure the amount of internalized ^{188}Re by cells.

In Vivo Animal Modal and Imaging: Female BALB/C mice were obtained from Nanjing Peng Sheng Biological Technology Co. Ltd. and used under protocols approved by the Soochow University Laboratory Animal Center. For tumor model, 2×10^6 4T1 cells concentrated in 50 μL PBS were subcutaneously injected into the right buttock of each mouse. SPECT imaging was conducted for

tumor-bearing mice after i.v. injection with 200 μL ^{188}Re-WS_2-PEG (1 mCi), using a U-SPECT+/CT from milabs.

Blood Circulation and Biodistribution Measurement: The radiolabeled ^{188}Re-WS_2-PEG (dose = 20 mg kg^{-1}, 200 μCi of ^{188}Re per mouse) or free ^{188}Re (200 μCi) was i.v. injected into the mice. The blood samples were taken from mice at various time points p.i. (15 min, 30 min, 1 h, 2 h, 4 h, 8 h, 12 h, 24 h, and 48 h), weighed, and then measured by the gamma counter to determine the radioactivity levels in the blood. For biodistribution, ^{188}Re-WS_2-PEG (dose = 20 mg kg^{-1}, 200 μCi of ^{188}Re per mouse) or free ^{188}Re (200 μCi) were i.v. injected into 4T1 tumor bearing mice. After 24 h, those mice were sacrificed and their organs including heart, liver, spleen, lung, kidney, skin, muscle, bone, and tumor were taken, weighed and measured by the gamma counter.

In Vivo Combined Therapy: Mice-bearing 4T1 tumors were divided into six groups (n = 5 per group) for various treatments including control group, mice i.v. injection with free ^{188}Re (200 μCi, 200 μL), WS_2-PEG (2 mg mL^{-1}, 200 μL, dose = 20 mg kg^{-1}) or ^{188}Re-WS_2-PEG (200 μCi, 200 μL). The above treatments were given by i.v. injection of various agents into mice bearing 4T1 tumors on day 0. For in vivo PTT, mice 24 h post i.v. injection with WS_2-PEG or ^{188}Re-WS_2-PEG were exposed to the 808-nm NIR laser (Hi-Tech Optoelectronics Co., Ltd. Beijing, China) at power density of ≈0.3 W cm^{-2} to maintain the tumor temperature at about 45–46 °C for 20 min. The tumor surface temperatures were recorded by an IR thermal camera (IRS E50 Pro Thermal Imaging Camera). After various treatments, the tumor sizes were measured by a vernier caliper every 2 d and calculated as the volume = (length × width^2)/2. Relative tumor volumes were calculated as V/V_0 (V_0 was the tumor volume when the treatment was initiated). On the other hand, tumors tissue and main organs from all six treated group were collected 1 d post treatment for H&E and TUNEL staining and examined by a fluorescence microscope (Olympus).

Immunohistochemistry: Mice-bearing 4T1 tumor were i.v. injected with WS_2-PEG nanoflakes. 24 h p.i., the tumor was irradiated with 808-nm laser at ≈0.3 W cm^{-2} for 20 min. After PTT, mice were intraperitoneal injected with nitroimidazole immediately. 90 min p.i., the tumors were collected, sliced, and stained with 2-(4-Amidinophenyl)-6-indolecarbamidine dihydrochloride (DAPI) (blue), anti-CD31 antibody (red), and anti-pimonidazole antibody (green), for cell nuclei, blood vessels, and hypoxia areas, respectively.

Supporting Information

Supporting Information is available from the Wiley Online Library or from the author.

Acknowledgements

This work was partially supported by the National Basic Research Programs of China (973 Program) (2012CB932600), the National Natural Science Foundation of China (51525203, 51572180, 81471716 and 31400861), the Juangsu Natural Science Fund (BK20130005 and BK20140320), Collaborative Innovation Center of Suzhou Nano Science and Technology, and a Project Funded by the Priority Academic Program Development (PAPD) of Jiangsu Higher Education Institutions.

[1] a) L. Cheng, C. Wang, L. Feng, K. Yang, Z. Liu, *Chem. Rev.* **2014**, *114*, 10869; b) D. Peer, J. M. Karp, S. Hong, O. C. FaroKhzad, R. Margalit, R. Langer, *Nat. Nanotechnol.* **2007**, *2*, 751.

[2] a) M. Sadeghi, M. Enferadi, A. Shirazi, *J. Cancer Res. Ther.* **2010**, *6*, 239; b) Z. Liu, J. Huang, C. Dong, L. Cui, X. Jin, B. Jia, Z. Zhu, F. Li, F. Wang, *Mol. Pharm.* **2012**, *9*, 1409.

[3] a) H. B. Stone, C. N. Coleman, M. S. Anscher, W. H. McBride, *Lancet Oncol.* **2003**, *4*, 529; b) C. Zhang, K. L. Zhao, W. B. Bu, D. L. Ni, Y. Y. Liu, J. W. Feng, J. L. Shi, *Angew. Chem. Int. Ed.* **2015**, *54*, 1770.

[4] a) S. D. Bao, Q. L. Wu, R. E. McLendon, Y. L. Hao, Q. Shi, A. B. Hjelmeland, M. W. Dewhirst, D. D. Bigner, J. N. Rich, *Nature* **2006**, *444*, 756; b) Y. Suh, S. J. Lee, *Arch. Pharm. Res.* **2015**, *38*, 408; c) M. Shrivastav, L. P. De Haro, J. A. Nickoloff, *Cell Res.* **2008**, *18*, 134.

[5] H. E. Barker, J. T. E. Paget, A. A. Khan, K. J. Harrington, *Nat. Rev. Cancer* **2015**, *15*, 409.

[6] a) X. R. Sun, X. F. Li, J. Russell, L. G. Xing, M. Urano, G. C. Li, J. L. Humm, C. C. Ling, *Radiother. Oncol.* **2008**, *88*, 269; b) M. R. Horsman, J. Overgaard, *Clin. Oncol.-UK* **2007**, *19*, 418; c) E. L. Jones, L. R. Prosnitz, M. W. Dewhirst, P. K. Marcom, P. H. Hardenbergh, L. B. Marks, D. M. Brizel, Z. Vujaskovic, *Clin. Cancer Res.* **2004**, *10*, 4287.

[7] a) N. R. Datta, S. G. Ordonez, U. S. Gaipl, M. M. Paulides, H. Crezee, J. Gellermann, D. Marder, E. Puric, S. Bodis, *Cancer Treat. Rev.* **2015**, *41*, 742; b) P. Wachsberger, R. Burd, A. P. Dicker, *Clin. Cancer Res.* **2003**, *9*, 1957; c) W. P. Fan, B. Shen, W. B. Bu, X. P. Zheng, Q. J. He, Z. W. Cui, D. L. Ni, K. L. Zhao, S. J. Zhang, J. L. Shi, *Biomaterials.* **2015**, *69*, 89; d) T. M. Pawlik, K. Keyomarsi, *Int. J. Radiat. Oncol.* **2004**, *59*, 928.

[8] F. Chen, H. Hong, Y. Zhang, H. F. Valdovinos, S. Shi, G. S. Kwon, C. P. Theuer, T. E. Barnhart, W. Cai, *ACS Nano* **2013**, *7*, 9027.

[9] a) T. Stylianopoulos, R. K. Jain, *Nanomed.: Nanotechnol.* **2015**, *11*, 1893; b) Z. Liu, W. Cai, L. He, N. Nakayama, K. Chen, X. Sun, X. Chen, H. Dai, *Nat. Nanotechnol.* **2007**, *2*, 47; c) R. Singh, D. Pantarotto, D. McCarthy, O. Chaloin, J. Hoebeke, C. D. Partidos, J.-P. Briand, M. Prato, A. Bianco, K. Kostarelos, *J. Am. Chem. Soc.* **2005**, *127*, 4388.

[10] a) X. Yi, K. Yang, C. Liang, X. Zhong, P. Ning, G. Song, D. Wang, C. Ge, C. Chen, Z. Chai, Z. Liu, *Adv. Funct. Mater.* **2015**, *25*, 4689; b) L. Chen, X. Zhong, X. Yi, M. Huang, P. Ning, T. Liu, C. Ge, Z. Chai, Z. Liu, K. Yang, *Biomaterials.* **2015**, *66*, 21.

[11] a) Q. F. Xiao, X. P. Zheng, W. B. Bu, W. Q. Ge, S. J. Zhang, F. Chen, H. Y. Xing, Q. G. Ren, W. P. Fan, K. L. Zhao, Y. Q. Hua, J. L. Shi, *J. Am. Chem. Soc.* **2013**, *135*, 13041; b) X. D. Zhang, J. Chen, Y. Min, G. B. Park, X. Shen, S. S. Song, Y. M. Sun, H. Wang, W. Long, J. P. Xie, K. Gao, L. F. Zhang, S. J. Fan, F. Y. Fan, U. Jeong, *Adv. Funct. Mater.* **2014**, *24*, 1718; c) G. Song, C. Liang, H. Gong, M. Li, X. Zheng, L. Cheng, K. Yang, X. Jiang, Z. Liu, *Adv. Mater.* **2015**, *27*, 6110.

[12] a) X.-D. Zhang, Z. Luo, J. Chen, X. Shen, S. Song, Y. Sun, S. Fan, F. Fan, D. T. Leong, J. Xie, *Adv. Mater.* **2014**, *26*, 4565; b) K. T. Butterworth, S. J. McMahon, F. J. Currell, K. M. Prise, *Nanoscale* **2012**, *4*, 4830; c) J. F. Hainfeld, F. A. Dilmanian, D. N. Slatkin, H. M. Smilowitz, *J. Pharm. Pharmacol.* **2008**, *60*, 977.

[13] a) Q. H. Wang, K. Kalantar-Zadeh, A. Kis, J. N. Coleman, M. S. Strano, *Nat. Nanotechnol.* **2012**, *7*, 699; b) G. C. Xu, Z. X. Lu, Q. Zhang, H. L. Qiu, L. Y. Jiao, *Acta Chim. Sinica* **2015**, *73*, 895; c) H. Zhang, *ACS Nano* **2015**, *9*, 9451; d) T. Liu, Z. Liu, *Acta Chim. Sinica* **2015**, *73*, 902.

[14] C. Tan, H. Zhang, *J. Am. Chem. Soc.* **2015**, *137*, 12162.

[15] a) H. Nam, B. R. Oh, P. Y. Chen, M. K. Chen, S. J. Wi, W. J. Wan, K. Kurabayashi, X. G. Liang, *Sci. Rep.* **2015**, *5*, 10546; b) K. Kalantar-zadeh, J. Z. Ou, T. Daeneke, M. S. Strano, M. Pumera, S. L. Gras, *Adv. Funct. Mater.* **2015**, *25*, 5086; c) J. Lu, J. H. Lu, H. Liu, B. Liu, L. Gong, E. S. Tok, K. P. Loh, C. H. Sow, *Small* **2015**, *11*, 1792.
[16] a) T. Liu, C. Wang, X. Gu, H. Gong, L. Cheng, X. Shi, L. Feng, B. Sun, Z. Liu, *Adv. Mater.* **2014**, *26*, 3433; b) T. Liu, C. Wang, W. Cui, H. Gong, C. Liang, X. Shi, Z. Li, B. Sun, Z. Liu, *Nanoscale* **2014**, *6*, 11219.
[17] a) L. Cheng, J. Liu, X. Gu, H. Gong, X. Shi, T. Liu, C. Wang, X. Wang, G. Liu, H. Xing, W. Bu, B. Sun, Z. Liu, *Adv. Mater.* **2014**, *26*, 1886; b) G. Yang, H. Gong, T. Liu, X. Sun, L. Cheng, Z. Liu, *Biomaterials.* **2015**, *60*, 62; c) Q. Tian, F. Jiang, R. Zou, Q. Liu, Z. Chen, M. Zhu, S. Yang, J. Wang, J. Wang, J. Hu, *ACS Nano* **2011**, *5*, 9761.
[18] T. Liu, S. Shi, C. Liang, S. Shen, L. Cheng, C. Wang, X. Song, S. Goel, T. E. Barnhart, W. Cai, Z. Liu, *ACS Nano* **2015**, *9*, 950.
[19] L. Cheng, C. Yuan, S. Shen, X. Yi, H. Gong, K. Yang, Z. Liu, *ACS Nano* **2015**, *9*, 11090.
[20] a) F. Chen, S. Goel, H. F. Valdovinos, H. Luo, R. Hernandez, T. E. Barnhart, W. Cai, *ACS Nano* **2015**, *9*, 7950; b) H. Hong, K. Yang, Y. Zhang, J. W. Engle, L. Feng, Y. Yang, T. R. Nayak, S. Goel, J. Bean, C. P. Theuer, T. E. Barnhart, Z. Liu, W. Cai, *ACS Nano* **2012**, *6*, 2361.
[21] F. F. Knapp, *Cancer Biother. Radio.* **1998**, *13*, 337.
[22] a) X. Y. Zhang, J. Li, Y. Zhu, Y. J. Qi, Z. Y. Zhu, W. X. Li, Q. Huang, *Nucl. Sci. Technol.* **2011**, *22*, 99; b) F. F. Knapp, A. L. Beets, S. Guhlke, P. O. Zamora, H. Bender, H. Palmedo, H. J. Biersack, *Anticancer. Res.* **1997**, *17*, 1783; c) J. Q. Cao, Y. X. Wang, J. F. Yu, J. Y. Xia, C. F. Zhang, D. Z. Yin, U. O. Hafeli, *J. Magn. Magn. Mater.* **2004**, *277*, 165.
[23] a) C. W. Song, A. Shakil, J. L. Osborn, K. Iwata, *Int. J. Hyperther.* **2009**, *25*, 91; b) K. F. Chu, D. E. Dupuy, *Nat. Rev. Cancer* **2014**, *14*, 199.
[24] L. Cheng, W. Huang, Q. Gong, C. Liu, Z. Liu, Y. Li, H. Dai, *Angew. Chem. Int. Ed.* **2014**, *53*, 7860.
[25] a) K. Yang, L. Feng, X. Shi, Z. Liu, *Chem. Soc. Rev.* **2013**, *42*, 530; b) K. Yang, J. M. Wan, S. Zhang, B. Tian, Y. J. Zhang, Z. Liu, *Biomaterials.* **2012**, *33*, 2206; c) J. T. Robinson, S. M. Tabakman, Y. Y. Liang, H. L. Wang, H. S. Casalongue, D. Vinh, H. J. Dai, *J. Am. Chem. Soc.* **2011**, *133*, 6825.
[26] a) R. T. M. de Rosales, C. Finucane, J. Foster, S. J. Mather, P. J. Blower, *Bioconjugate. Chem.* **2010**, *21*, 811; b) C. Dong, H. Zhao, S. Yang, J. Shi, J. Huang, L. Cui, L. Zhong, X. Jin, F. Li, Z. Liu, B. Jia, F. Wang, *Mol. Pharm.* **2013**, *10*, 2925.
[27] Y. Yong, X. Cheng, T. Bao, M. Zu, L. Yan, W. Yin, C. Ge, D. Wang, Z. Gu, Y. Zhao, *ACS Nano* **2015**, *9*, 12451.
[28] A. Al Zaki, D. Joh, Z. L. Cheng, A. L. B. De Barros, G. Kao, J. Dorsey, A. Tsourkas, *ACS Nano* **2014**, *8*, 104.
[29] G. Song, C. Liang, X. Yi, Q. Zhao, L. Cheng, K. Yang, Z. Liu, *Adv. Mater.* **2016**, *28*,2716.
[30] Z. Liu, S. M. Tabakman, Z. Chen, H. Dai, *Nat. Protocols* **2009**, *4*, 1372.

Received: April 21, 2016
Revised: May 27, 2016
Published online: June 27, 2016